International Journal of Biometeorology (2026) 70:8
https://doi.org/10.1007/s00484-025-03109-w

ORIGINAL PAPER

Quantifying associations between local climate zones on land surface temperature: new insights from coastal areas of Italy

Oznur Isinkaralar[1] · Kaan Isinkaralar[2] · Dilara Yilmaz[3] · Emmanuel Yeboah[4] · Isaac Sarfo[5,6] · Sevgi Öztürk[1]

Received: 5 May 2025 / Revised: 22 September 2025 / Accepted: 2 October 2025 / Published online: 3 January 2026

Abstract

Coastal regions across Europe face rising sea levels and climate change-related extreme weather conditions such as more frequent and intense heat waves, floods, droughts, and storms. As climate change and rapid urbanization continue to pose significant challenges to the resilience of cities, knowledge from LCZ studies has the potential to generate targeted adaptation strategies that address the unique thermal performance characteristics of different urban areas. A range of physical characteristics, such as the density and type of buildings, the presence of vegetation and the amount of impervious surface, defines local climatic zones. The study focuses on the change in LCZ classification (1 to 10 and A to G) between 2003 and 2023 and its relationship with LST. The most pronounced increase occurred in LCZ3 (compact low-rise), with an expansion of 139 km², equivalent to more than a tenfold (1158%) rise from its 2003 extent. It was found that areas classified as LCZD (low plants) in 2003 were transformed into LCZ9 (sparsely built areas) in 2023. The transformation of vegetated areas into urban areas in the study area demonstrates the striking impact of urbanization over the last 20 years.

Keywords Adaptation strategies · Climate action · Climate crisis · Environmental challenges · Life on land

Introduction

The prediction that urbanization will increase highlights the need for comprehensive research on urban planning strategies in reducing the impact of urban fabric on the urban environment, especially the increase in surface temperatures (Reis and Lopes 2019; Vandamme et al. 2019; Yang et al. 2020). As urbanization continues to accelerate globally, understanding the spatial patterns of thermal performance in cities has become increasingly important to address climate change adaptation measures (Oliveira et al. 2020; Yenigun et al. 2025). Land cover patterns strongly influence urban local climate. This forms the basis for creating a land cover map based on the microclimate characteristics of a city (Shi et al. 2018). The ongoing urban development has revealed the need for new methods and searches to standardize research on urban climate.

Climate zones, which are defined by the patterns of temperature, precipitation, and other meteorological factors, play a crucial role in shaping the physical and social environments across the globe (Weaver et al. 2017; Aydin et al. 2025). Recent studies have emphasized the importance of using local climate zones (LCZ) parameters to investigate urban microclimates and ventilation conditions (He et al. 2015; Zhang et al. 2021). As a result of this need, the LCZ classification developed by Stewart and Oke (2012) is a frequently used method in studies that allows the evaluation of the local climate of cities within

✉ Oznur Isinkaralar
obulan@kastamonu.edu.tr

1 Department of Landscape Architecture, Faculty of Engineering and Architecture, Kastamonu University, Kastamonu 37150, Türkiye

2 Department of Environmental Engineering, Faculty of Engineering and Architecture, Kastamonu University, Kastamonu 37150, Türkiye

3 Department of Landscape Architecture, Graduate School of Natural and Applied Sciences, Kastamonu University, Kastamonu 37150, Türkiye

4 School of Remote Sensing and Geomatics Engineering, Nanjing University of Information Science and Technology, Nanjing 210044, Jiangsu, China

5 College of Geography and Environmental Science, Henan University, Kaifeng, Henan Province, China

6 Organization of African Academic Doctors (OAAD), Off Kamiti Road, P. O. Box 25305000100, Nairobi, Kenya

the scope of specific land use and land cover (LULC) characteristics. Climate Zones has become a standard method for categorizing urban areas' land cover and land use characteristics in relation to their corresponding climatic influences (Ren et al. 2010; Back et al. 2021). It is used in studies on urban morphology and urban heat island (Zhao et al. 2020; Cao et al. 2022; Xiang et al. 2023), in studies focusing on the effect of LCZ changes on land surface temperature (LST) in urban areas (Mushore et al. 2022a), and in studies focusing on the classification of urban areas (Bechtel et al. 2015; Demuzere et al. 2021). The impacts of climate change on these climate zones are well-documented, with studies showing that warming temperatures are leading to shifts in precipitation patterns, sea level rise, and the increased frequency and intensity of extreme weather events (Ondiko et al. 2022). To date, many studies have examined the relationship between LCZ and LST in many cities around the world (Khoshnoodmotlagh et al. 2021; Zwolska et al. 2024). In these studies, it has been shown that these complementary data sources provide a powerful additional resource for urban planning by integrating with LCZ and LST within the scope of urban heat island and urban morphology detection (Xu et al. 2017; Isinkaralar et al. 2025a, b). These changes are having far-reaching consequences on both the natural and built environments, with coastal regions facing the risk of flooding and inland areas experiencing the effects of droughts, heatwaves, and wildfires (Schmidt et al. 2021; Huser et al. 2022). The literature review has also highlighted the need for a more risk-based approach to climate change assessments, as managing these risks will be crucial in mitigating the negative impacts on communities and ecosystems (Alexander 2020; Chen et al. 2020). By identifying and evaluating specific risks, their likelihood, and potential consequences, policymakers and stakeholders can develop more effective strategies to promote resilience and adaptation in these challenges (Danylo et al. 2016; Das and Das 2020).

Considering all these, the main objectives of this study are to investigate the relationship between LCZ and LST in coastal cities of Italy by determining the impact of impervious density (IMD) and the transformation between LCZs on LST over a 20-year period (2003–2023). Specifically, this study aims to answer the following research questions:

(1) Which LCZ types are dominant in the coastal cities of Italy?
(2) Which LCZ types have a statistically higher correlation with LST values?
(3) How can LCZ changes over time be assessed in the context of climate risk?

Materials and methods

Study area

The analysis in this research was carried out in 4 different coastal cities of Italy (Liguria, Tuscany, Emilia-Romagna, Veneto), one of the important countries of Europe. The study area covers a total area of 136,005 km². The climate characteristics of Italy are incredibly diverse. Although the typical Mediterranean climate is dominant in most of the country according to the geographical characteristics of the region, there are climatic differences. While the inner northern regions of Italy are in the hot summer (Cfa) category of the Köppen climate classification, that is, in a temperate climate zone, the part covering the study area is no dry season and warm summer (Cfb), Cfa, and warm summer (Csb) categories (Fig. 1).

Method

Figure 2 illustrates the procedural framework used in the study. The study was conducted in 3 main stages. First, MODIS LST data were obtained, and LST analysis was performed. Then, IMD analysis was performed and the relationship between LST and IMD was analyzed with the linear regression model. LCZ classification was performed with the bands of Landsat 5 and Landsat 8 satellite images using the WUDAPT procedure. The average LST values in each of the classifications were calculated and the LST changes in the LCZ classes were analyzed.

Retrieval of LST from the MODIS data

The study used the MOD11A2v6 product (1 km spatial resolution) from the Terra MODIS collection to determine LST over the 20 years between 2003 and 2023. MODIS LST data were obtained from NASA database (MoDIS Land 2023). MODIS data were converted from MODIS units to LST in degrees Celsius by applying the MODIS scale factor. In the LST calculation, the annual average LST was calculated by calculating a 4-month average LST for each year, January, May, August, and October, representing the seasonal situation of the study area. Finally, the MODIS satellite image has a spatial resolution of 1 km. However, to obtain more effective results in analysis and evaluation, the resulting LST map was produced at 100*100 m, which aligns with the LCZ map target resolution. The "project raster" tool in the ArcGIS 10.4.1 program was used to adjust the resolution of the map. Then, MODIS LST data were divided into 2 periods as 2003–2012 (LST_{M1}) and 2013–2023 (LST_{M2}). All the differences in LST values and LCZ changes were found to be statistically significant at the $p<0.001$ level.

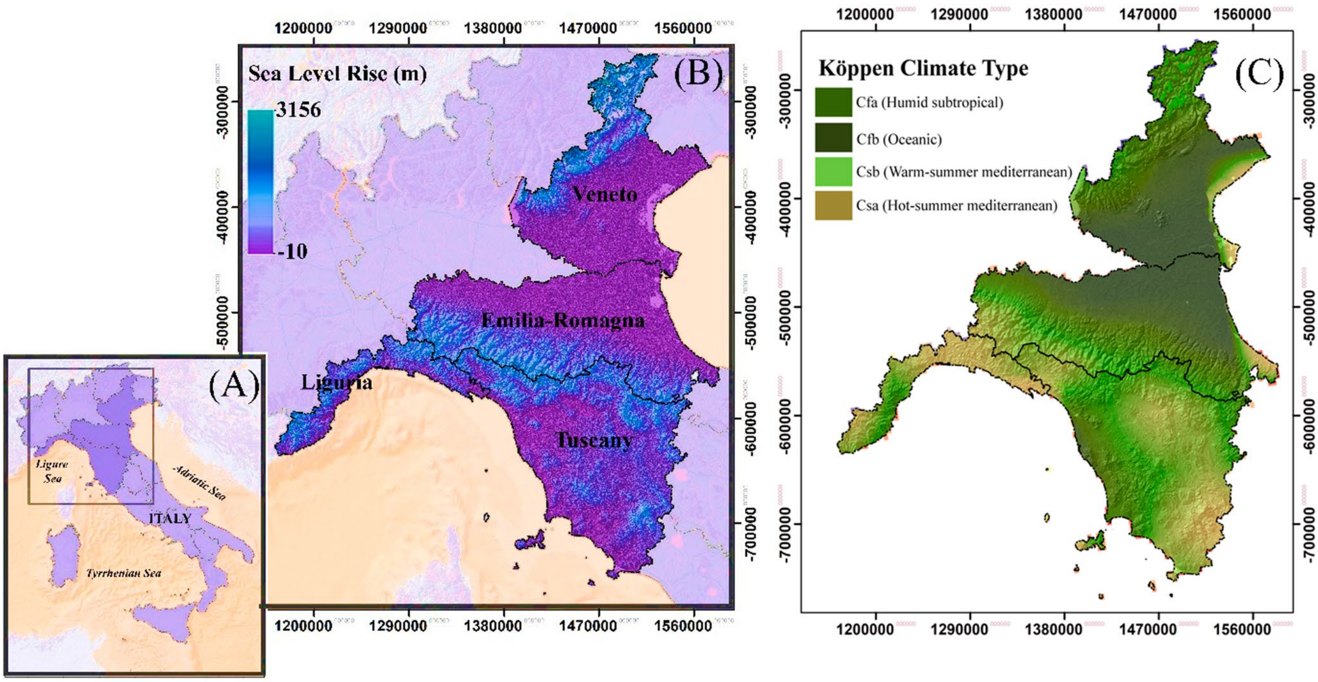

Fig. 1 The research area location maps **A**: Coastal zone of Italy, **B**: Study area, **C**: Köppen climate types of Italy (climate types calculated from data from WorldClim Global Climate Data platform (Xu and Hutchinson 2011)

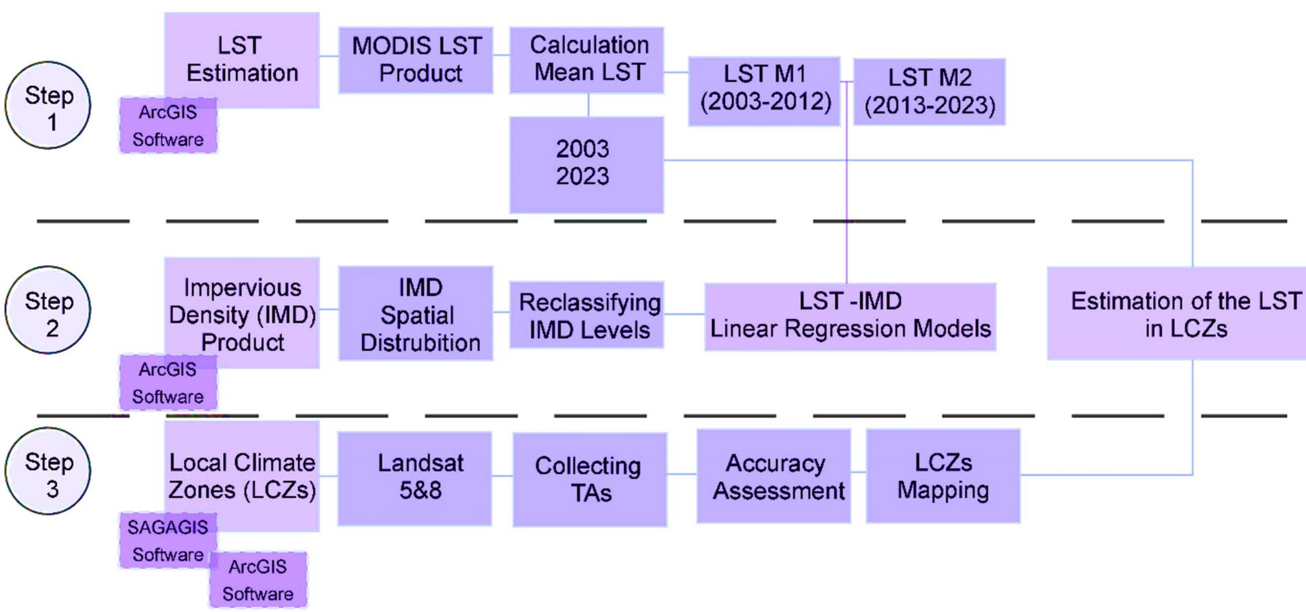

Fig. 2 Flowchart of the data collection and analysis of the study

Furthermore, a strong correlation was observed between the rates of change in LCZ classes and the rates of LST change.

Imperviousness of surface

In the study, 2009 and 2018 IMD products from the Copernicus database (EEA 2025) were used to determine how impermeable surfaces affect LST in the 20 years between 2003 and 2023. IMD products were produced for 3 years using a semi-automatic classification based on the Normalized Difference Vegetation Index (NDVI). IMD is available at 100 m spatial resolution for the reference years 2006, 2009, 2012, 2015, and 2018 (EEA 2024).

The IMD product with 100 m resolution has been successfully used in studies on mapping local climates of urban areas together with the LCZ classification by Demuzere et al. (2019). Within the scope of the research, daytime LST MOD11A2v6 Terra MODIS data from 2003 to 2023 and IMD data from 2009 (3-year product of the 2008–2010 temporal scope) and 2018 (3-year product of the 2017–2019 temporal scope) were used. The changes in the percentage of impermeable areas between 2006 and 2018, together with the LST between the two selected periods, were investigated. The relationship between IMD and LST was analyzed using a linear regression model. To facilitate the spatial and numerical evaluation of IMD distributions, IMD values were divided into five groups: Grup1: %0–20, Grup2: %21–40, Grup3: %41–60, Grup4: %61–80, and Grup5: %81–100.

LCZ classification using LCZ generator

The WUDAPT LCZ procedure was applied to determine the LCZ classes for Italy. The procedure steps were performed using Google Earth, SAGA GIS, and ArcGIS programs. The LCZ procedure completed the pre-processing processes of Landsat satellite images and satellite raster data. Then, the training areas (TAs) were digitized. Finally, the classification algorithm was applied in SAGA GIS. In order to perform the LCZ classification with the WUDAPT procedure, cloudless satellite images corresponding to 4 seasons were obtained from the Landsat 5.7 ETM and Landsat 8 OLI/TIRS satellites of the United States Geological Survey (USGS) according to the seasonal characteristics of the study area. The satellite images were combined by making a mosaic, then clipped within the study area boundaries and made ready for classification. Bands 1–7 of the satellite images were used for LCZ classification (Table 1).

Table 1 Landsat images used in LCZs classification

Image Acquisition Date	Sensor	Bands for LCZ Classification
20.01.2003–27.01.2003	Landsat 7 ETM	1–7
26.05.2003–28.05.2003		
17.08.2003–24.08.2003	Landsat 5 ETM	
11.10.2003–20.10.2003.10.2003		
31.01.2012	Landsat 7 ETM	1–7
27.05.2012–29.05.2012		
22.08.2012–24.08.2012		
18.10.2012–25.10.2012.10.2012		
18.01.2013–23.01.2013	Landsat 8 OLI/TIRS	1–7
22.05.2013–29.05.2013		
19.08.2013–26.08.2013		
15.10.2013–22.10.2013.10.2013		
18.01.2023–27.01.2023	Landsat 8 OLI/TIRS	1–7
25.05.2023–27.05.2023		
22.08.2023–24.08.2023		
24.10.2023–27.10.2023.10.2023		

After obtaining satellite images for the years 2003 and 2023, digitized TAs were collected according to WUDAPT guidelines from locations with unchanged LULC categories. The TAs were initially collected in Google Earth software and saved in kml format. They were subsequently converted into shp format using ArcGIS for SAGA-GIS. The Landsat satellite images obtained for the years 2003 and 2023 were resampled to 100-meter resolution (Yoo et al. 2019). To ensure pixel compatibility in the analyses, LCZ data were resampled at 100 m resolution using the resampling tool (Grid-Tools-Module Resampling) in the SAGA GIS program. Then, the classification algorithm was applied in SAGA GIS to create the LCZ classification based on the resampled Landsat satellite images and the selected training areas. The algorithm used in the WUDAPT procedure is a Random Forest (RF) classifier (Bechtel et al. 2019).

It consists of decision trees that assign each image pixel to the LCZ type. Since its subsets are randomly formed, it is called RF. While RF provides valuable results, it requires a small amount of training data and also manages to process large amounts of data without any capacity. It is preferred for GIS data and multi-source remote sensing datasets (Rodriguez-Galiano et al. 2012; Choe and Yom 2020; Mushore et al. 2022b).

The overall accuracy metrics across all cities were evaluated based on their averages. While city-specific models are recommended by WUDAPT, in this study a regional model was adopted to ensure temporal consistency across 2003–2023. The relatively lower overall accuracy (OA) in 2003 (61.59%) is attributed to the limitations of the satellite data rather than the classification approach. The calculated accuracy values for the LCZ map of the city are given in Table 2. According to the data in Table 2, the 2003 LCZ classification achieved an overall accuracy value of 61.59 and a kappa value of 0.64, while the 2023 LCZ classification reached an OA value of 71.69 and a kappa value of 0.72. In 2003, the producer's accuracy values ranged from 40.59% to 89.11%, and the user's accuracy values ranged from 48.59% to 81.08%. In 2023, the PA values fell between 51.47% and 89.99%, and the UA values were within the range of 59.15% to 87.87%. The average UA and PA values of the 2003 and 2023 are consistent with other studies in the literature. Ren et al. (2019) reported an overall distribution of LCZ maps between 60% and 89% across countries, with a standard deviation of 76% and 7.2%. Johnson and Jozdani (2019) calculated the OA of the LCZ map to be 0.76, while producer's accuracy (PA) values range from 0.06 to 1.0 and user's accuracy (UA) values range from 0.03 to 1.0. In their study, Bechtel et al. (2020) reported an OA value of 0.59. These studies support the reliability of LCZ classifications in capturing urban heat dynamics.

Table 2 LCZ transfer matrix of the study area (2003–2023)

LCZs		UA (%)	PA (%)	Overall Accuracy (%)	Kappa
2003	2	51.16	58.85	**61.59**	**0.64**
	3	59.97	65.47		
	5	48.59	40.59		
	6	69.89	71.75		
	8	71	74.01		
	9	65.05	69		
	10	68.19	77.98		
	A	80.79	80.65		
	B	87	86.01		
	C	69.98	79.75		
	D	72.74	67.71		
	E	60.96	68		
	F	61.68	71		
	G	81.08	89.11		
2023	1	71.25	70.54	**71.69**	**0.72**
	2	59.15	68.85		
	3	61.79	51.47		
	4	61.41	68.56		
	5	69.99	66.78		
	6	73.79	75.65		
	7	74.35	76.51		
	8	74.04	76.55		
	9	69.58	71.41		
	10	77.191	79.98		
	A	85.86	86.98		
	B	81.82	89.78		
	C	74.89	79.75		
	D	71.74	84.98		
	E	86.98	87		
	F	77.77	71.65		
	G	87.87	89.99		

Table 3 Changes of areas (km²) IMD levels between 2009 and 2018

IMD Level	IMD 2009	IMD 2018	Change of area	Change of average LST (°C)
1: %0–20	53.292	42.632	−10.660	−6.78
2: %21–40	2842	4973	+2131	+3.04
3: %41–60	2131	3553	+1422	+5
4: %61–80	5684	9237	+3553	+7.2
5: %81–100	7105	10.659	+3554	+9.8

Results and discussion

Relationship between the IMD and LST

When comparing the IMDs of 2009 and 2018, IMD level 1 (%0–20) shows the highest decrease, with a significant drop in value. At the same time, IMD level 5 (%81–100) shows the highest increase, indicating that the most disadvantaged areas have seen the most significant rise in IMD over this period. At the same time, regardless of the change in IMD levels, the highest increase in LST values is seen in IMD level 5 with 9.8 °C (Table 3). As supported by several recent studies, the increase in urban land surface temperature (LST) is primarily driven by both local urbanization and global climate change. Stowell et al. (2023) emphasize that urban green spaces and local development patterns significantly influence LST in cities worldwide, highlighting the role of vegetation in mitigating urban heat. In a case study of Lagos, a rapidly growing metropolis in West Africa, Guo et al. (2022) demonstrate that urban expansion and global climate change significantly contribute to LST increases, with urban morphology and building density being the primary factors. Similarly, García and Rezapouraghdam (2023) show that climate change and urban structuring in Seville influence heat stress variability, suggesting that city-scale planning can mitigate local thermal impacts.

When examining the spatial pattern of IMD levels, it is observed that they tend to increase particularly in the northwestern parts of the study area, especially in its interior regions (Fig. 3).

The linear regression analysis results determining the relationship between LST and IMD are presented in Fig. 4. The analysis results indicate a positive relationship between IMD and LST. Increased impervious surface density causes a rise in LST values. According to the linear regression analysis between 2009 IMD and LST_{M1}, the increase in 2009 IMD explained 48% of LST_{M1}, while the linear regression analysis between 2018 IMD and LST_{M2} showed that the increase in 2018 IMD explained 87% of LST_{M2}.

Relationship between the LCZs and LST

The research maps created using SAGA GIS and ArcGIS programs show the 20-year urbanization process of the study area. The study area has experienced a spatial change in local climate zones in land surface temperature, particularly in the inner regions. These urban areas have seen an increase in the low vegetation cover class. The spread of urban areas has intensified the urban heat island effect (Li et al. 2021; Mo et al. 2024). Areas with predominantly concrete and asphalt, which absorb heat, such as housing and commercial structures, have contributed to the formation of the urban heat island. In other words, identifying and classifying local climate zones is an important tool for climate-focused planning and design in urban areas, including mitigating the urban heat island (Liu et al. 2020; Soward and Li 2021) (Figure 5).

Between 2003 and 2023, the highest increase in urban areas was observed in LCZ3. The most significant decrease in urban areas was seen in LCZ6. There was generally a decline in natural areas, with the most substantial decrease observed in LCZD (Fig. 6; Table 4).

The study area has generally transitioned from low-vegetation areas to urban areas from 2003 to 2023. The results

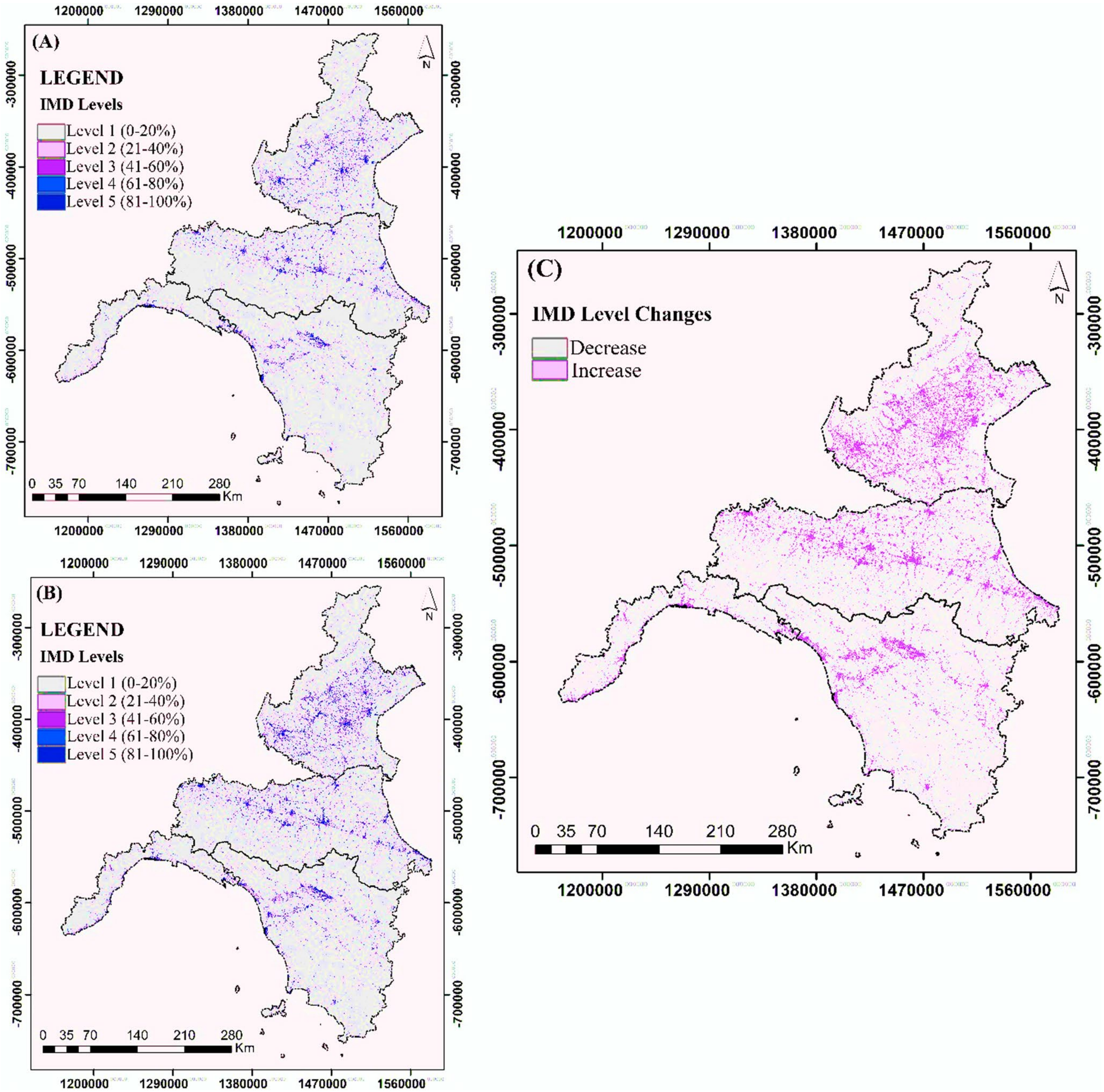

Fig. 3 Spatial distributions of IMD levels and changes of IMD levels between 2009 and 2018 (**A**: 2009, **B**: 2018, **C**: IMD levels changes)

presented in Table 4 indicate that areas classified as LCZD in 2003 have been transformed into LCZ9 areas by 2023. This conversion of vegetation-covered areas to urban areas reflects the impact of urbanization over the past 20 years.

According to the LST maps shown in Fig. 7, the land surface temperatures in the study area have increased significantly from 2003 to 2023. In 2003, the LST values ranged from 13.05 °C to 35.51 °C, but by 2023, these values had risen to between 16.55 °C and 40.75 °C. The presence of high LST values even in the coastal regions of the study area indicates that excessive warming is one of the most prominent signs of the changing climate in this urban environment.

The most extreme land surface temperature levels are observed within urban local climate zones, where the built environment and human activities contribute to forming distinct microclimates. In contrast, more moderate LST values are characteristic of natural LCZs, such as forested areas and open spaces, less influenced by anthropogenic factors (Mouzourides et al. 2019). Historical data show that in 2003, LST in natural LCZs typically remained below 25 °C. However, these levels have since risen above that threshold

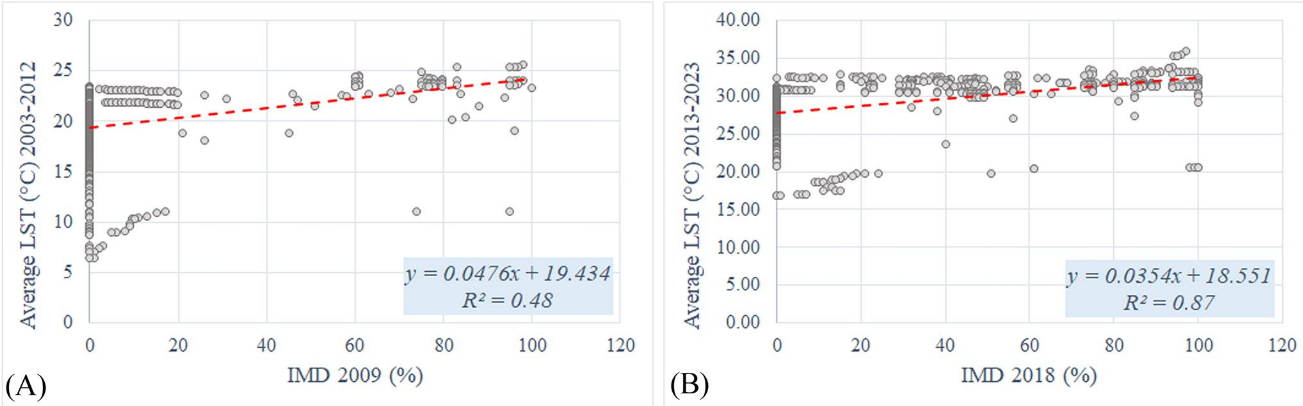

Fig. 4 Linear regression models, the relationship between IMD and LST (A: IMD 2009 and LST_{M1}, B: IMD 2018 and LST_{M2})

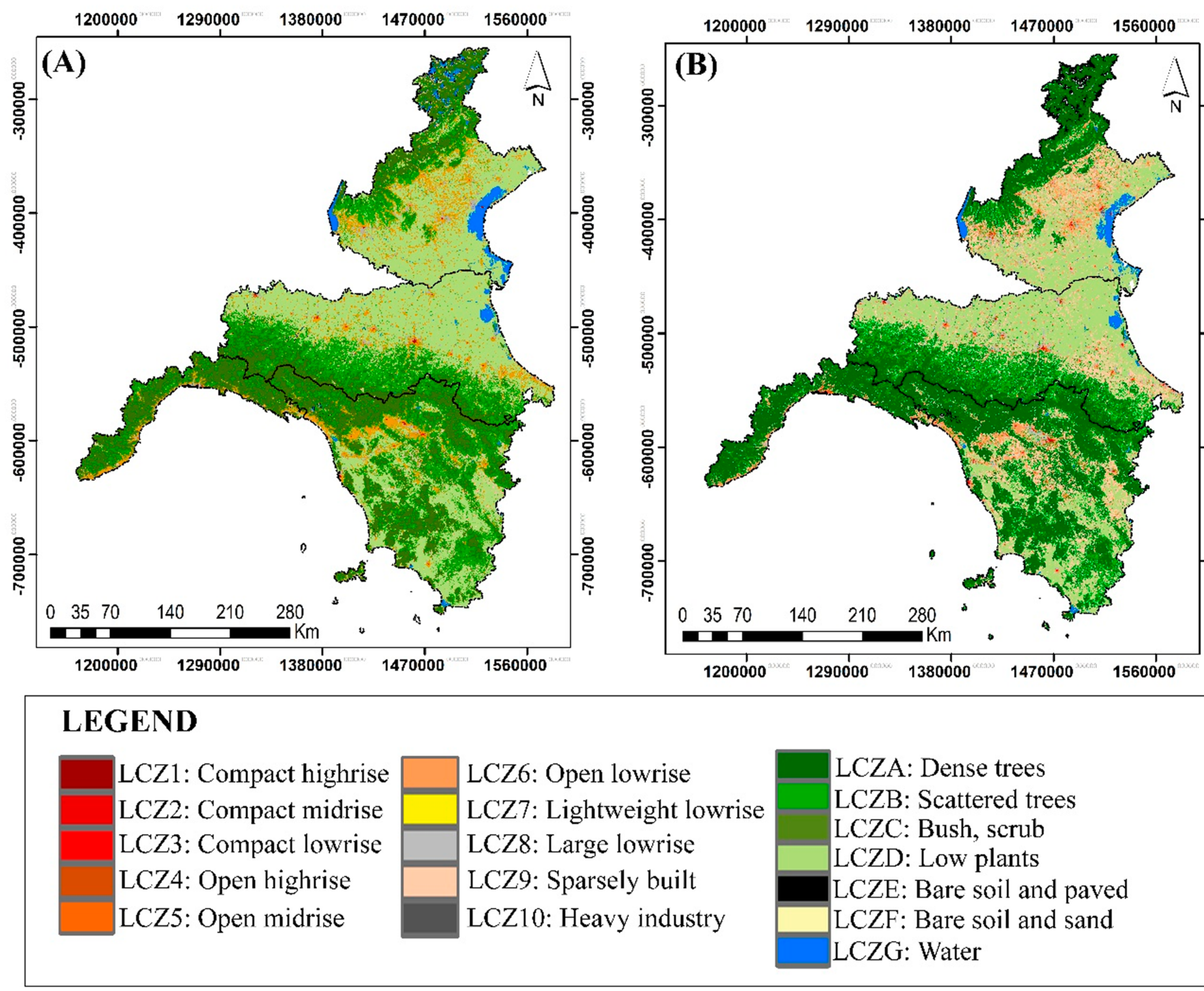

Fig. 5 Maps of study area LCZs (A: 2003, B: 2023)

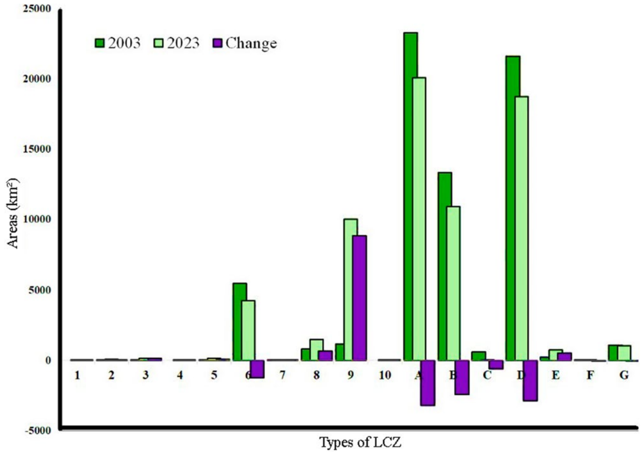

Fig. 6 Changes in the area of LCZs between 2003 and 2023

by 2023, indicating significant thermal warming has also occurred in these areas. This trend highlights the growing importance of understanding and addressing the impacts of local climate zones on urban environments and the need for targeted mitigation and adaptation strategies (Fig. 8).

Over the past 20 years, from 2003 to 2023, urban local climate zones have exhibited higher average, median, maximum, and minimum land surface temperature values, which are closely linked to land use patterns. The various land cover configurations significantly determine the increase in LST values. Notably, natural LCZs, particularly LCZG with water bodies, have experienced lower increases in maximum and minimum LST values. The largest magnitudes of statistical changes were observed in the classes that underwent the most substantial transformations. These findings highlight the significance of understanding and monitoring local climate zones in urban areas, as they play a crucial role in shaping the thermal environment and have important implications for urban planning, climate adaptation, and environmental management (Table 5).

To further isolate the contribution of urbanization from the background climate signal, we subtracted the mean climate-driven ΔLST estimated from unchanged natural LCZs (LCZG and LCZF). Table 6 then reports the resulting urban-induced ΔLST values for the urban LCZ classes. The table includes only urban LCZs and shows that compact built-up classes exhibit markedly higher urban-induced warming: LCZ1 and LCZ10 present the largest excess ΔLST values (16.39 °C and 13.26 °C, respectively). Other urban classes show substantially smaller urban-induced increases (e.g., LCZ2 = 1.58 °C; LCZ3 = 0.66 °C; LCZ4 = 5.56 °C; LCZ8 = 3.10 °C). These results indicate that, although regional climate warming affects all LCZs, the excess warming attributable to urbanization is most pronounced in compact built-up areas.

The spatial autocorrelation analysis revealed that both LCZ and LST exhibited significant clustering patterns in 2003 and 2023 (Table 7). In 2003, Moran's I values were 0.644 for LCZ and 0.622 for LST, while in 2023 these values increased to 0.734 and 0.776, respectively ($p < 0.001$ for all cases). This indicates that spatial dependence in both urban form and land surface temperature has become stronger over time. Ordinary Least Squares (OLS) regression further showed that LCZs explained a substantial proportion of the variance in LST values. The adjusted R^2 value was 0.51 in 2003 and increased to 0.64 in 2023, suggesting that the explanatory power of LCZs on LST has strengthened over the two decades. In both models, the coefficients were statistically significant ($p < 0.001$), standard errors remained low, and variance inflation factor (VIF) values (2003: 3.19; 2023: 2.60) indicated no multicollinearity problems. Collectively, these results demonstrate that the spatial clustering of LCZs and LST has intensified, and the relationship between urban morphology and surface temperature has become more pronounced between 2003 and 2023.

Urbanization in coastal cities across Europe has accelerated over the past two decades, significantly altering the local urban morphology. Accurate and up-to-date urban morphological data are crucial for understanding the spatial variability of urban climate and for generating reliable local climate maps. This study proposes a satellite-based approach to map LCZs and assess their relationship with LST over a 20-year period. By integrating LCZ classification with temporal satellite imagery, the methodology provides a robust framework for evaluating the thermal impacts of urban expansion and the transformation of vegetated areas into built-up zones. A comparison of different built-up class types within the LCZ classification revealed that configuration patterns play a significant role in modifying the LST. Built-up classes, such as compact high-rise buildings and fragmented green spaces, increase the LST, while less compact areas, such as open mid-rise buildings and sparsely built-up buildings with more green space, decrease the LST. Analysis shows that compact LCZs (especially LCZs 2 and 3) have the highest surface temperatures, while densely vegetated LCZ types (e.g., LCZs D, A, B) have a significant cooling effect on the LST. Some studies show a pivotal role in mitigating heat of greenspaces, trees and vegetation in urban areas (Yu et al. 2024, 2025; Zhou et al. 2025a, b).

Our results indicate that compact high-rise (LCZ1) and heavy industry (LCZ10) exhibit the strongest urban-induced warming (+16.36 °C and +13.26 °C, respectively), which may translate into 30–80% higher heat-related mortality risk during extreme events. Extreme heat events are well-documented to increase mortality rates, particularly in densely populated urban areas (Coates et al. 2014; Gasparrini et al. 2015; Vicedo-Cabrera et al. 2021; Masselot et al. 2025). Our

Table 4 Transformation of LCZs classes between 2003 and 2023 (km^2)

		2023																	
		LCZ1	LCZ2	LCZ3	LCZ4	LCZ5	LCZ6	LCZ7	LCZ8	LCZ9	LCZ10	LCZA	LCZB	LCZC	LCZD	LCZE	LCZF	LCZG	Sum
2003	LCZ1	0	0	0	0	0	0	0	0	0	0	0	0	0	0	0	0	0	0
	LCZ2	1.11	29	0	0	0	20.17	0	0	0	0	0	0	0	1.72	0	0	0	52
	LCZ3	1.31	9	1.69	0	0	0	0	0	0	0	0	0	0	0	0	0	0	12
	LCZ4	0	0	0	0	0	0	0	0	0	0	0	0	0	0	0	0	0	0
	LCZ5	0	0.18	0	0	21	19.18	0	0	0	0	0	0	0	0	0	1.64	0	42
	LCZ6	5.38	21	0	4	1	3967.78	0	1385	0	0	0	0	0	85.49	9.87	10.19	14.15	5503.86
	LCZ7	0	0.21	0.17	0.18	0	0	0	0	0	0	0	0	0	0	0	0	0	0.56
	LCZ8	0	0	131	0	0	103	12.18	98.74	0	0	0	114.15	0	321.87	0	0	53.06	834
	LCZ9	0	0	5.31	0	0	21	0	0	987.71	18.66	0	0	0	103.32	0	0	0	1136
	LCZ10	0	0	0	0	0	0	0	0	0	0	0	0	0	0	0	0	0	0
	LCZA	0	0	0	0	78	0	0	0	0	0	19,052	0	0	4146	0	0	0	23,276
	LCZB	0	0	0	4.7	0	87.23	0	0	13.17	0	0	10423.13	0	2786.44	9.33	0	0	13,324
	LCZC	0	0	0	0	0	0	0	0	453.01	0	0	119.87	26	11.12	0	0	0	610
	LCZD	0	8.61	12.83	18.12	31	15.86	4.82	7.26	8350.23	7.13	1021.89	120.72	0	11179.27	599.87	16.58	190.08	21584.27
	LCZE	0	0	0	0	0	0	0	0	48.5	1.21	0	0	0	61.29	121	0	0	232
	LCZF	0	0	0	0	0	0	0	0	0	0	0	0	0	21.48	9.93	16.59	0	48
	LCZG	0	0	0	0	0	9.78	0	2	143.38	0	0	121.13	0	0	0	0	787.71	1064
	Sum	7.8	68	151	27	131	4244	21.44	1493	9996	27	20,024	10,899	26	18,718	750	45	1045	67,719

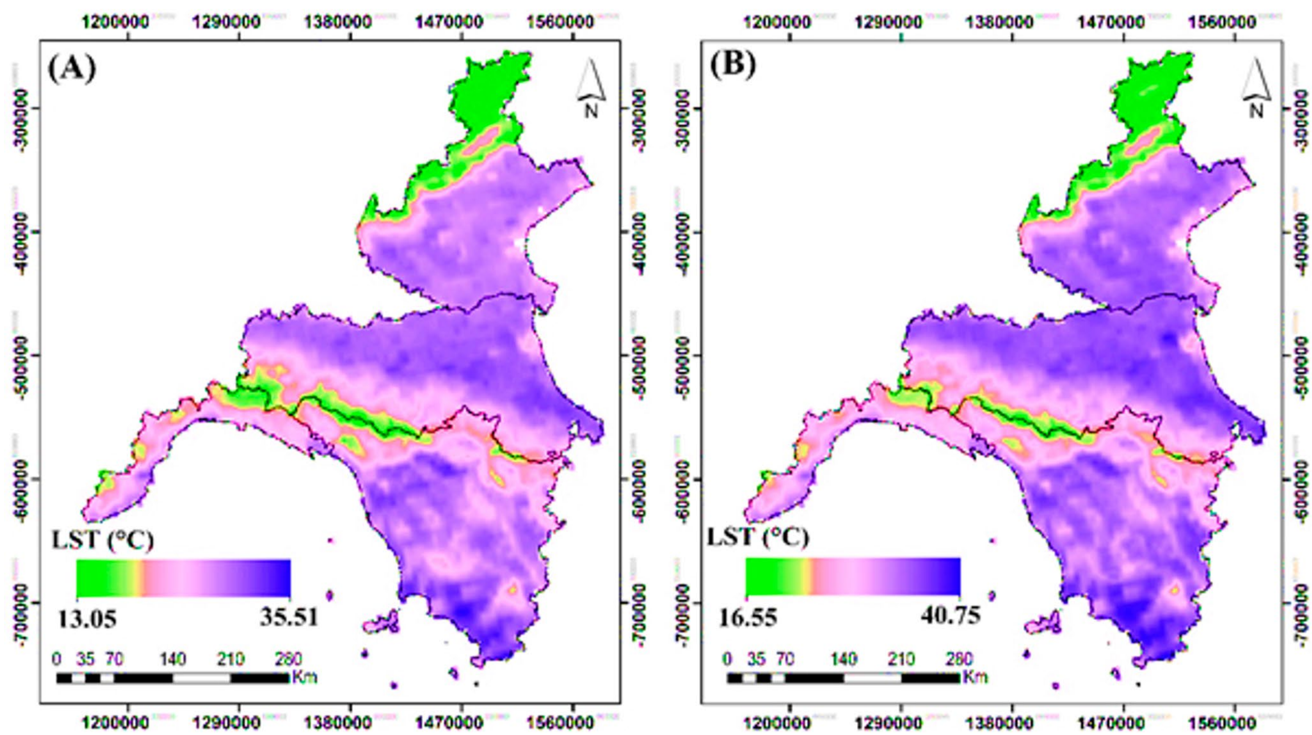

Fig. 7 Study area average LST (**A**: 2003, **B**: 2023)

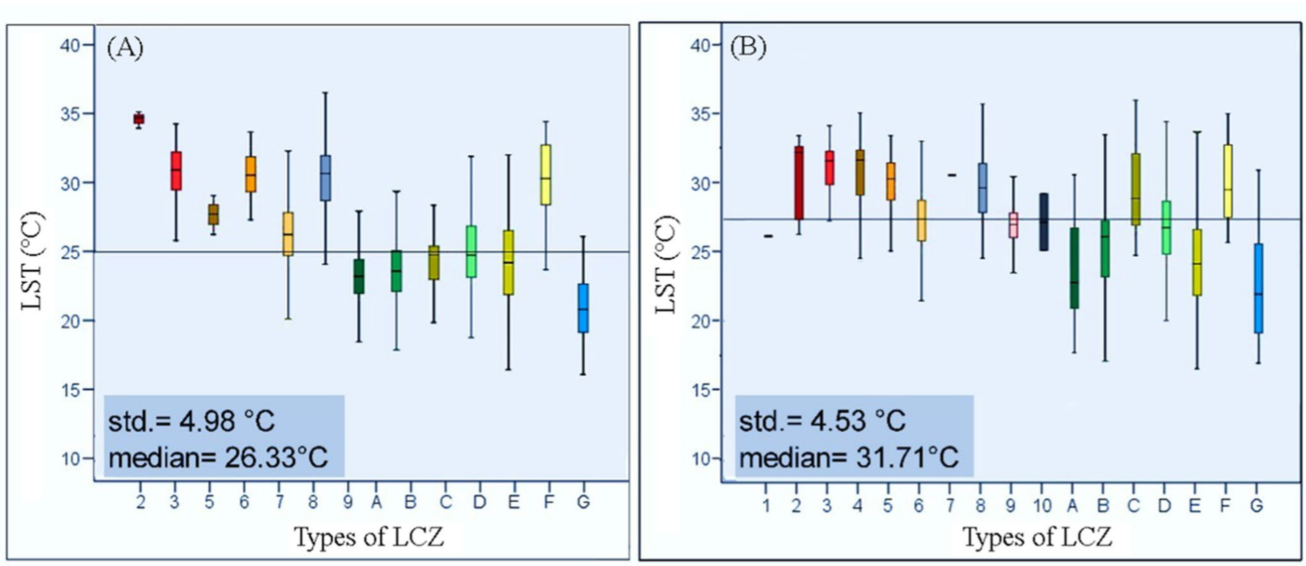

Fig. 8 Study area average LST in LCZs (**A**: 2003, **B**: 2023)

results indicate that compact high-rise (LCZ1) and heavy industry (LCZ10) exhibit the strongest urban-induced warming (+16.36 °C and +13.26 °C, respectively), which may translate into substantial increases in heat-related morbidity and mortality. Based on empirical evidence, policy targets should be more specific: achieving ≥ 30% tree canopy cover in LCZ1 has been shown to significantly reduce LST peaks in neighborhoods during heatwaves (Endreny et al. 2025), and reaching approximately 30–40% canopy cover in compact urban contexts yields up to approximately 4–5 °C surface cooling (Wang et al. 2019; Ren et al. 2022). Similarly, raising surface albedo of impervious materials (e.g., pavements) above ~0.3–0.5 can deliver large surface cooling effects (Elgendy et al. 2025). Therefore, we propose applicable thresholds for our study area: (1) increasing tree canopy cover to ≥30% in the most affected LCZs (LCZ1,

Table 5 Changes in the mean LST (°C) between periods 2003–2023 and according to LCZ classes

LCZ Type	Mean LST	Median LST	Max LST	Min LST	*r*
LCZ1	17.51	8.97	18.17	27.88	0.97
LCZ2	2.73	2.75	5.41	3.24	0.81
LCZ3	1.81	1.78	4.12	4.12	0.90
LCZ4	6.71	3.23	9.88	4.73	0.44
LCZ5	4.23	1.88	10.12	3.78	0.53
LCZ6	3.32	1.96	9.72	2.69	0.21
LCZ7	2.12	2.47	8.61	4.72	0.12
LCZ8	4.25	3.68	7.60	5.69	0.13
LCZ9	2.19	2.47	3.19	4.46	0.15
LCZ10	14.41	6.45	11.87	18.78	0.87
LCZA	1.11	1.13	1.01	1.09	0.51
LCZB	1.20	1.32	4.21	1.87	0.63
LCZC	1.71	1.69	5.15	1.77	0.35
LCZD	1.45	1.51	4.25	1.69	0.38
LCZE	1.30	1.41	3.69	0.96	0.41
LCZF	1.05	1.09	4.32	0.12	0.68
LCZG	1.25	1.65	0.58	0.97	0.71

$p < 0.001$,r: Correlation coefficient

Table 6 Urban heating between 2003–2023 and by LCZ classes

LCZ Type	Mean LST	Urban-induced ΔLST (°C)
LCZ1	17.51	16.36
LCZ2	2.73	1.58
LCZ3	1.81	0.66
LCZ4	6.71	5.56
LCZ5	4.23	3.08
LCZ6	3.32	2.17
LCZ7	2.12	0.97
LCZ8	4.25	3.10
LCZ9	2.19	1.04
LCZ10	14.41	13.26

LSTclimate= (LCZFmeanLST + LCZGmeanLST)/2

Urban-induced ΔLST = ΔLST – LST climate(1.15)

LCZ10), (2) reducing impervious surface cover in these LCZs by 20–30%, and (3) ensuring that impervious surface and roof materials achieve an albedo value of ≥0.3, especially in LCZ4–LCZ8. Implementation of these measures could reduce urban-induced ΔLST by ~2–3 °C in LCZ1 and by ~1–2 °C in medium-density urban LCZs, resulting in a corresponding reduction in heat-related risk.

While many studies report a consistent pattern of higher surface temperatures in compact built LCZ classes, LCZ-thermal rankings are not universal and may vary across cities and climate contexts. Several studies have shown that LCZ thermal contrasts are strongly influenced by macroclimate, coastal effects, and local morphology. Recent multi-city assessments also demonstrate variation in which LCZs register the highest LST values, depending on factors such as building materials, height-to-width ratios, and proximity to large water bodies (Zwolska et al. 2024; Manyanya et al. 2024; Parvar et al. 2024). These mixed results suggest that simple generalisations are not valid everywhere. In our coastal study area, maritime forcing mechanisms including sea breezes, higher humidity, and the thermal inertia of adjacent water bodies plausibly alter LCZ thermal ordering compared with inland mid-latitude cities.

Consequently, these findings are consistent with the results of previous studies reporting temperature differences between LCZ classes in other urban areas (Stewart et al. 2014; Leconte et al. 2015; Shi et al. 2018; Mushore et al. 2019; Alexander 2020; Khoshnoodmotlagh et al. 2021). The study also revealed that the transformation of natural and semi-natural areas (LCZ D) into densely built-up LCZ classes (LCZ 3, LCZ 9) in a coastal city during the period 2003–2023 led to a significant increase in surface temperature (LST), especially in the thermal environment. This trend is consistent with recent studies highlighting the increase in LST as natural areas are converted into buildings in urbanized regions (Xiao et al. 2022; Mushore et al. 2022a, b; Mengistu et al. 2025).

These results demonstrate that increasing heat stress in coastal cities is closely linked not only to global climate change but also to local morphological transformations. In this context, LCZ-based analyses offer a critical tool for developing strategies to mitigate the urban heat island effect by protecting vegetation, reducing impervious surfaces, and promoting shading-enhancing urban forms. Our study is one of the first to systematically document the impacts of LCZ transformations on LST in coastal cities, providing data directly applicable to both urban planning and the design of climate change adaptation strategies.

Conclusion

The findings of this study strengthen the evidence that explores the significance of utilizing LCZ to assess climate risk and urbanization dynamics in urban areas. The LCZ framework offers a standardized approach to classify urban landscapes according to climate-relevant surface

Table 7 Global Moran I index and OLS analysis results

Variables		Moran's I	Z-Score	Adj.R^2	S.D	T-Value	*p*-value	VIF
2003	LCZ	0.644	36.98	0.51	0.003	10.462	0.00	3.191
	LST	0.622	35.727					
2023	LCZ	0.734	42.139	0.64	0.004	10.563	0.00	2.600
	LST	0.776	44.508					

characteristics, enabling a more detailed understanding of the complex relationships between the built environment and local climatic conditions. Integrating LCZ mapping with the multi-resolution analysis of urban canopy parameters has emerged as a tool for investigating urban microclimates and identifying priority areas for intervention. As climate change and rapid urbanization continue to pose significant challenges to the resilience of cities, information from LCZ investigations can provide insights to inform the development of targeted adaptation strategies that address the unique thermal performance characteristics of different urban areas. Urban planners and policy makers can better understand the spatial distribution of thermal performance in a city, enabling them to optimize the application of climate change adaptation measures and promote the overall sustainability and resilience of urban communities by applying LCZ mapping and analysis. As the world increasingly becomes more urbanized, the use of LCZ research will continue to play an essential role in supporting the development of more livable, climate-resilient cities.

Acknowledgements Not applicable.

Authors' contributions Oznur Isinkaralar: Processing analysis, interpretation, original draft, data curation, review & editing. Kaan Isinkaralar: Processing analysis, interpretation, original draft, data curation. Dilara Yilmaz: Processing analysis, data curation, writing – review & editing. Emmanuel Yeboah: Processing analysis, interpretation, original draft, data curation. Isaac Sarf: Writing – review & editing. Sevgi Öztürk: Writing – review & editing.

Funding There is no financial support and commercial support.

Data availability The data that support the findings of this study are available from the corresponding author, upon reasonable request.

Declarations

Ethics approval All authors have read, understood, and have complied as applicable with the statement on "Ethical responsibilities of Authors" as found in the Instructions for Authors.

Consent to participate Not applicable.

Consent to publish Not applicable.

Conflict of interest The authors declare that they have no conflict of interest.

References

Alexander C (2020) Normalised difference spectral indices and urban land cover as indicators of land surface temperature (LST). Int J Appl Earth Obs Geoinf 86:102013. https://doi.org/10.1016/j.jag.2019.102013

Aydin H, Yenigun K, Isinkaralar O, Isinkaralar K (2025) Resilience to drought-affected areas in a semi-arid agricultural watershed by climate risk: practical implications for sub-basin scale case. Pure Appl Geophys. https://doi.org/10.1007/s00024-025-03794-z

Back Y, Bach PM, Jasper-Tönnies A, Rauch W, Kleidorfer M (2021) A rapid fine-scale approach to modelling urban bioclimatic conditions. Sci Total Environ 756:143732. https://doi.org/10.1016/j.scitotenv.2020.143732

Bechtel B, Alexander PJ, Böhner J, Ching J, Conrad O, Feddema J, Mills G, See L, Stewart I (2015) Mapping local climate zones for a worldwide database of the form and function of cities. ISPRS Int J Geo-Inf 4(1):199–219. https://doi.org/10.3390/ijgi4010199

Bechtel B, Demuzere M, Mills G, Zhan W, Sismanidis P, Small C, Voogt J (2019) SUHI analysis using Local Climate Zones—a comparison of 50 cities. Urban Clim 28:100451. https://doi.org/10.1016/j.uclim.2019.01.005

Bechtel B, Demuzere M, Stewart ID (2020) A weighted accuracy measure for land cover mapping: comment on Johnson et al. local climate zone (LCZ) map accuracy assessments should account for land cover physical characteristics that affect the local thermal environment. Remote Sens. 2019, 11, 2420. Remote Sens 12(11):1769. https://doi.org/10.3390/rs12111769

Cao Q, Huang H, Hong Y, Huang X, Wang S, Wang L, Wang L (2022) Modeling intra-urban differences in thermal environments and heat stress based on local climate zones in central Wuhan. Build Environ 225:109625. https://doi.org/10.1016/j.buildenv.2022.109625

Chen X, Xu Y, Yang J, Wu Z, Zhu H (2020) Remote sensing of urban thermal environments within local climate zones: a case study of two high-density subtropical Chinese cities. Urban Clim 31:100568. https://doi.org/10.1016/j.uclim.2019.100568

Choe YJ, Yom JH (2020) Improving accuracy of land surface temperature prediction model based on deep-learning. Spat Inf Res 28:377–382. https://doi.org/10.1007/s41324-019-00299-5

Coates L, Haynes K, O'brien J, McAneney J, De Oliveira FD (2014) Exploring 167 years of vulnerability: an examination of extreme heat events in Australia 1844–2010. Environ Sci Policy 42:33–44. https://doi.org/10.1016/j.envsci.2014.05.003

Danylo O, See L, Bechtel B, Schepaschenko D, Fritz S (2016) Contributing to WUDAPT: a local climate zone classification of two cities in Ukraine. IEEE J Sel Top Appl Earth Observations Remote Sens 9(5):1841–1853. https://doi.org/10.1109/JSTARS.2016.2539977

Das M, Das A (2020) Assessing the relationship between local climatic zones (LCZs) and land surface temperature (LST)–a case study of Sriniketan-Santiniketan Planning Area (SSPA), West Bengal, India. Urban Clim 32:100591. https://doi.org/10.1016/j.uclim.2020.100591

Demuzere M, Bechtel B, Middel A, Mills G (2019) Mapping Europe into local climate zones. PLoS One 14(4):e0214474. https://doi.org/10.1371/journal.pone.0214474

Demuzere M, Kittner J, Bechtel B (2021) LCZ generator: a web application to create Local Climate Zone maps. Front Environ Sci 9:637455. https://doi.org/10.3389/fenvs.2021.637455

EEA (2024) Imperviousness. European Union https://land.copernicus.eu/en/products/high-resolution-layer-imperviousness(accessed on 12 January 2025)

EEA (2025) High Resolution Layers, © European Union, Copernicus Land Monitoring Service 2025; European Environment Agency (EEA). Available online: https://land.copernicus.eu/pan-european/high-resolution-layers/ (accessed on 11 January 2025)

Elgendy D, Tolba O, Kamel T (2025) The impact of increasing urban surface albedo on outdoor air and surface temperatures during summer in newly developed areas. Sci Rep 15(1):25165. https://doi.org/10.1038/s41598-025-08574-2

Endreny TA, Ciolfi M, Endreny A, Chiocchini F, Calfapietra C (2025) Neighborhood-scale reductions in heatwave burden projected under a 30% minimum tree cover scenario. Npj Urban Sustain 5(1):50. https://doi.org/10.1038/s42949-025-00219-7

García DH, Rezapouraghdam H (2023) Variability of heat stress using the urbclim climate model in the City of Seville (Spain): mitigation proposal. Environ Monit Assess 195(10):1164. https://doi.org/10.1007/s10661-023-11768-8

Gasparrini A, Guo Y, Hashizume M, Kinney PL, Petkova EP, Lavigne E, Zanobetti A, Schwartz JD, Tobias A, Leone M, Tong S, Honda Y, Kim H, Armstrong BG (2015) Temporal variation in heat–mortality associations: a multicountry study. Environ Health Perspect 123(11):1200–1207. https://doi.org/10.1289/ehp.1409070

Guo L, Di L, Zhang C, Lin L, Chen F, Molla A (2022) Evaluating contributions of urbanization and global climate change to urban land surface temperature change: a case study in Lagos, Nigeria. Sci Rep 12(1):14168. https://doi.org/10.1038/s41598-022-18193-w

He X, Shen S, Miao S, Dou J, Zhang Y (2015) Quantitative detection of urban climate resources and the establishment of an urban climate map (UCMap) system in Beijing. Build Environ 92:668–678. https://doi.org/10.1016/j.buildenv.2015.05.044

Huser R, Hazra A, Bolin D (2022) Realistic and Fast Modeling of Spatial Extremes over Large Geographical Domains. In EGU General Assembly Conference Abstracts (pp. EGU22-6595). https://doi.org/10.5194/egusphere-egu22-6595

Isinkaralar O, Isinkaralar K, Yilmaz D, Öztürk S (2025a) Multi-dimensional analysis of land use/land cover and urbanization on seasonal variation of land surface temperature in İzmir, Türkiye. Landsc Ecol Eng 21(1):133–150. https://doi.org/10.1007/s11355-024-00628-3

Isinkaralar O, Yeboah E, Isinkaralar K, Sarfo I, Öztürk S, Yilmaz D, Bojago E (2025b) Investigating the effects of local climate zones on land surface temperature using spectral indices via linear regression model: a seasonal study of Sapanca lake. Environ Monit Assess 197(3):252. https://doi.org/10.1007/s10661-025-13705-3

Johnson BA, Jozdani SE (2019) Local climate zone (LCZ) map accuracy assessments should account for land cover physical characteristics that affect the local thermal environment. Remote Sens 11(20):2420. https://doi.org/10.3390/rs11202420

Khoshnoodmotlagh S, Daneshi A, Gharari S, Verrelst J, Mirzaei M, Omrani H (2021) Urban morphology detection and it's linking with land surface temperature: a case study for Tehran Metropolis, Iran. Sustain Cities Soc 74:103228. https://doi.org/10.1016/j.scs.2021.103228

Leconte F, Bouyer J, Claverie R, Pétrissans M (2015) Using local climate zone scheme for UHI assessment: evaluation of the method using mobile measurements. Build Environ 83:39–49. https://doi.org/10.1016/j.buildenv.2014.05.005

Li N, Yang J, Qiao Z, Wang Y, Miao S (2021) Urban thermal characteristics of local climate zones and their mitigation measures across cities in different climate zones of China. Remote Sens 13(8):1468. https://doi.org/10.3390/rs13081468

Liu P, Jia S, Han R, Liu Y, Lu X, Zhang H (2020) RS and GIS supported urban LULC and UHI change simulation and assessment. J Sens 2020(1):5863164. https://doi.org/10.1155/2020/5863164

Manyanya T, Nethengwe NS, Verbist B, Somers B (2024) Optimizing local climate zones through clustering for surface urban heat island analysis in building height-scarce cities: a cape town case study. Climate 12(9):142. https://doi.org/10.3390/cli12090142

Masselot P, Mistry MN, Rao S, Huber V, Monteiro A, Samoli E, Stafoggia M, de'Donato F, Garcia-Leon D, Carlos Ciscar J, Feyen L, Schneider A, Katsouyanni K, Vicedo-Cabrera AM, Aunan K, Gasparrini A (2025) Estimating future heat-related and cold-related mortality under climate change, demographic and adaptation scenarios in 854 European cities. Nat Med 31(4):1294–1302. https://doi.org/10.1038/s41591-024-03452-2

Mengistu AG, Tesfuhuney WA, Woyessa YE, Ejigu AA, Alemu MD (2025) Future climate and hydrological extremes in Ethiopia: a CMIP6-based analysis. Adv Meteorol 2025(1):5571487. https://doi.org/10.1155/adme/5571487

Mo N, Han J, Yin Y, Zhang Y (2024) Seasonal analysis of land surface temperature using local climate zones in peak forest basin topography: a case study of Guilin. Build Environ 247:111042. https://doi.org/10.1016/j.buildenv.2023.111042

MODIS Land MODIS Land Science Team https://modis-land.gsfc.nasa.gov/ (2023), accessed on 10 January 2025

Mouzourides P, Eleftheriou A, Kyprianou A, Ching J, Neophytou M (2019) Linking local-climate-zones mapping to multi-resolution-analysis to deduce associative relations at intra-urban scales through an example of Metropolitan London. Urban Climate 30:100505. https://doi.org/10.1016/j.uclim.2019.100505

Mushore TD, Dube T, Manjowe M, Gumindoga W, Chemura A, Rousta I, Odindi J, Mutanga O (2019) Remotely sensed retrieval of local climate zones and their linkages to land surface temperature in Harare metropolitan city, Zimbabwe. Urban Climate 27:259–271. https://doi.org/10.1016/j.uclim.2018.12.006

Mushore TD, Mutanga O, Odindi J (2022a) Understanding growth-induced trends in local climate zones, land surface temperature, and extreme temperature events in a rapidly growing city: a case of Bulawayo Metropolitan City in Zimbabwe. Front Environ Sci 10:1. https://doi.org/10.3389/fenvs.2022.910816

Mushore TD, Mutanga O, Odindi J (2022b) Determining the influence of long term urban growth on surface urban heat islands using local climate zones and intensity analysis techniques. Remote Sens 14:2060. https://doi.org/10.3390/rs14092060

Oliveira A, Lopes A, Niza S (2020) Local climate zones in five southern European cities: an improved GIS-based classification method based on Copernicus data. Urban Climate 33:100631. https://doi.org/10.1016/j.uclim.2020.100631

Ondiko JH, Karanja AM, Ombogo O (2022) A review of the anthropogenic effects of climate change on the physical and social environment. Open Access Libr J 9(2):1–14. https://doi.org/10.4236/oalib.1107751

Parvar Z, Mohammadzadeh M, Saeidi S (2024) LCZ framework and landscape metrics: exploration of urban and peri-urban thermal environment emphasizing 2/3D characteristics. Build Environ 254:111370. https://doi.org/10.1016/j.buildenv.2024.111370

Reis C, Lopes A (2019) Evaluating the cooling potential of urban green spaces to tackle urban climate change in Lisbon. Sustainability 11(9):2480. https://doi.org/10.3390/su11092480

Ren C, Ng E, Katzschner L (2010) Urban climatic map studies: a review. Int J Climatol 31(15):2213–2233. https://doi.org/10.1002/joc.2237

Ren C, Cai M, Li X, Zhang L, Wang R, Xu Y, Ng E (2019) Assessment of local climate zone classification maps of cities in China and feasible refinements. Sci Rep 9(1):18848. https://doi.org/10.1038/s41598-019-55444-9

Ren Z, Zhao H, Fu Y, Xiao L, Dong Y (2022) Effects of urban street trees on human thermal comfort and physiological indices: a case study in Changchun city, China. J Forestry Res 33(3):911–922. https://doi.org/10.1007/s11676-021-01361-5

Rodriguez-Galiano VF, Ghimire B, Rogan J, Chica-Olmo M, Rigol-Sanchez JP (2012) An assessment of the effectiveness of a random forest classifier for land-cover classification. ISPRS J Photogramm Remote Sens 67:93–104. https://doi.org/10.1016/j.isprsjprs.2011.11.002

Schmidt V, Luccioni AS, Teng M, Zhang T, Reynaud A, Raghupathi S, Cosne G, Juraver A, Vardanyan VR, Hernández-García Á, Bengio Y (2021) Climategan: Raising climate change awareness by generating images of floods. ArXiv Preprint arXiv 211002871. https://doi.org/10.48550/arxiv.2110.02871

Shi Y, Lau KKL, Ren C, Ng E (2018) Evaluating the local climate zone classification in high-density heterogeneous urban environment using mobile measurement. Urban Clim 25:167–186. https://doi.org/10.1016/j.uclim.2018.07.001

Soward E, Li J (2021) ArcGIS urban: an application for plan assessment. Comput Urban Sci 1(1):15. https://doi.org/10.1007/s43762-021-00016-9

Stewart ID, Oke TR (2012) Local climate zones for urban temperature studies. Bull Am Meteorol Soc 93(12):1879–1900. https://doi.org/10.1175/BAMS-D-11-00019.1

Stewart ID, Oke TR, Krayenhoff ES (2014) Evaluation of the'local climate zone'scheme using temperature observations and model simulations. Int J Climatol. https://doi.org/10.1002/joc.3746

Stowell J, Ngo C, Jimenez MP, Kinney PL, James P (2023) Development of a global urban greenness indicator dataset for 1,000+cities. Data Brief 48:109140. https://doi.org/10.1016/j.dib.2023.109140

Vandamme S, Demuzere M, Verdonck ML, Zhang Z, Van Coillie F (2019) Revealing kunming's (China) historical urban planning policies through local climate zones. Remote Sens 11(14):1731. https://doi.org/10.3390/rs11141731

Vicedo-Cabrera AM, Scovronick N, Sera F, Roye D, Schneider R, Tobias A, Astrom C, Guo Y, Honda Y, Hondula DM, Abrutzky R, Tong S, Coelho MSZS, Saldiva PHN, Lavigne E, Correa PM, Ortega NV, Kan H, Osorio S, Kysely J, Urban A, Orru H, Indermitte E, Jaakkola JJK, Ryti N, Pascal M, Schneider A, Katsouyanni K, Samoli E, Mayvaneh F, Entezari A, Goodman P, Zeka A, Michelozzi P, de Donato F, Hashizume M, Alahmad B, Diaz MH, Cdlc V, Overcenco A, Houthuijs D, Ameling C, Rao S, Di Ruscio F, Carrasco-Escobar G, Seposo X, Silva S, Madureira J, Holobaca IH, Fratianni S, Acquaotta F, Kim H, Lee W, Iniguez C, Forsberg B, Ragettli MS, Yll G, Chen BY, Li S, Armstrong B, Aleman A, Zanobetti A, Schwartz J, Dang TN, Dung DV, Gillett N, Haines A, Mengel M, Huber V, Gasparrini A (2021) The burden of heat-related mortality attributable to recent human-induced climate change. Nat Clim Chang 11(6):492–500. https://doi.org/10.1038/s41558-021-01058-x

Wang C, Wang ZH, Wang C, Myint SW (2019) Environmental cooling provided by urban trees under extreme heat and cold waves in US cities. Remote Sens Environ 227:28–43. https://doi.org/10.1016/j.rse.2019.03.024

Weaver C, Moss RH, Ebi KL, Gleick PH, Stern PC, Tebaldi C, Wilson RS, Árvai J (2017) Reframing climate change assessments around risk: recommendations for the US National Climate Assessment. Environ Res Lett 12(8):080201. https://doi.org/10.1088/1748-9326/aa7494

Xiang Y, Cen Q, Peng C, Huang C, Wu C, Teng M, Zhou Z (2023) Surface urban heat island mitigation network construction utilizing source-sink theory and local climate zones. Build Environ 243:110717. https://doi.org/10.1016/j.buildenv.2023.110717

Xiao R, Cao W, Liu Y, Lu B (2022) The impacts of landscape patterns spatio-temporal changes on land surface temperature from a multi-scale perspective: a case study of the Yangtze River Delta. Sci Total Environ 821:153381. https://doi.org/10.1016/j.scitotenv.2022.153381

Xu T, Hutchinson M (2011) ANUCLIM version 6.1 user guide. The Australian National University, Fenner School of Environment and Society, Canberra, p 90

Xu Y, Ren C, Ma P, Ho J, Wang W, Lau KKL, Lin H, Ng E (2017) Urban morphology detection and computation for urban climate research. Landsc Urban Plann 167:212–224. https://doi.org/10.1016/j.landurbplan.2017.06.018

Yang J, Wang Y, Xiu C, Xiao X, Xia J, Jin C (2020) Optimizing local climate zones to mitigate urban heat island effect in human settlements. J Clean Prod 275:123767. https://doi.org/10.1016/j.jclepro.2020.123767

Yenigun K, Bozkurt A, Isinkaralar O, Isinkaralar K (2025) Ancient karez systems in Şanlıurfa, Türkiye: detection, analysis, and sustainability of historical water supply networks. Spat Inf Res 33(3):22. https://doi.org/10.1007/s41324-025-00623-2

Yoo C, Han D, Im J, Bechtel B (2019) Comparison between convolutional neural networks and random forest for local climate zone classification in mega urban areas using Landsat images. ISPRS J Photogramm Remote Sens 157:155–170. https://doi.org/10.1016/j.isprsjprs.2019.09.009

Yu Z, Chen J, Chen J, Zhan W, Wang C, Ma W, Yao X, Zhou S, Zhu K, Sun R (2024) Enhanced observations from an optimized soil-canopy-photosynthesis and energy flux model revealed evapotranspiration-shading cooling dynamics of urban vegetation during extreme heat. Remote Sens Environ 305:114098. https://doi.org/10.1016/j.rse.2024.114098

Yu Z, Li S, Yang W, Chen J, Rahman MA, Wang C, Ma W, Yao X, Xiong J, Xu C, Zhou Y, Chen J, Huang K, Gao X, Fensholt R, Weng Q, Zhou W (2025) Enhancing climate-driven urban tree cooling with targeted nonclimatic interventions. Environ Sci Technol 59(18):9082–9092. https://doi.org/10.1021/acs.est.4c14275

Zhang Y, Zhang X, Xu W, Jiao B (2021), March A case study on urban ventilation assessment with local climate zone (LCZ) parameters. In IOP Conference Series: Earth and Environmental Science (Vol. 696, No. 1, p. 012033). IOP Publishing. https://doi.org/10.1088/1755-1315/696/1/012033

Zhao C, Jensen JL, Weng Q, Currit N, Weaver R (2020) Use of local climate zones to investigate surface urban heat islands in Texas. GIScience Remote Sens 57(8):1083–1101. https://doi.org/10.1080/15481603.2020.1843869

Zhou SQ, Yu ZW, Ma WY, Yao XH, Xiong JQ, Ma WJ, Xiang SY, Yuan Q, Hao YY, Xu DF, Wang BY, Zhao B (2025a) Vertical canopy structure dominates cooling and thermal comfort of urban pocket parks during hot summer days. Landsc Urban Plann 254:105242. https://doi.org/10.1016/j.landurbplan.2024.105242

Zhou SQ, Yu ZW, Wu WB, Yang WJ, Zhang YJ, Hao YY, Yuan Q, Xu DF, Hu JY, Zhao B (2025b) Quantifying cumulative cooling threshold of greenspaces using a newly developed 3D model across global cities. Remote Sens Environ 328:114867. https://doi.org/10.1016/j.rse.2025.114867

Zwolska A, Półrolniczak M, Kolendowicz L (2024) Urban growth's implications on land surface temperature in a medium-sized European city based on LCZ classification. Sci Rep 14(1):8308. https://doi.org/10.1038/s41598-024-58501-0